Vibrational spectra of acid and alkaline glycine salts

Mário T. Rosado [a], Maria Leonor T.S. Duarte [a], Rui Fausto [b],[*]

[a] *Departamento de Química e Bioquímica, Faculdade de Ciências da Universidade de Lisboa, Ed. C1-5°, Campo Grande, 1700 Lisbon, Portugal*
[b] *Departamento de Química, Universidade de Coimbra, 3049 Coimbra, Portugal*

Abstract

The infrared and Raman spectra of crystalline acid ($^+NH_3CH_2COOH \cdot Cl^-$) and alkaline ($Na^+ \cdot NH_2CH_2COO^-$) glycine salts were recorded and interpreted. The assignments were confirmed by comparison with the infrared and Raman spectra of crystalline glycine (zwitterion, $^+NH_3CH_2COO^-$) and the infrared spectrum of this molecule isolated in an argon matrix at low temperature (10 K) (neutral form, NH_2CH_2COOH). Further insight on the features of the vibrational spectra of these substances was achieved by ab initio (HF/6-31G*) frequency and intensity calculations and potential energy distribution calculations resulting from normal coordinate analysis. © 1998 Elsevier Science B.V.

Keywords: Glycine (neutral and zwitterionic forms); Acid and alkaline glycine salts; Vibrational (IR and Raman) spectra; Ab initio prediction of vibrational spectra

1. Introduction

Glycine is the simplest protein structural unit and the smallest amino acid that can act as neuroinhibitor in mammalian central nervous systems [1,2]. Since vibrational spectroscopy can provide the key to elucidation of both structural and dynamical properties and can be used to establish fundamental correlations between these and the chemical or biochemical behaviour of these substances, considerable effort has been dedicated to such studies on glycine under various experimental conditions [2–12]. Interesting vibrational features of the infrared spectra of glycine, both in the zwitterionic [2–9] and neutral forms

[10,11], have previously been studied, although the main focus has been on the zwitterion, due to its greater biological importance.

The assignment of bands in the infrared spectrum of crystalline glycine (zwitterion) presents difficulties, due to the presence of some regions with very broad and structured bands (e.g. νOH, νNH and νCH stretching regions). The study of the vibrational spectra of glycine alkaline and acid salts appeared to be a promising way of understanding complex features of the zwitterion spectra, since $-NH_2$, $-COO^-$ and $-COOH$, $-NH_3^+$ groups are present in alkaline and acid salts, respectively. However, glycine salts have not previously received much attention.

Williams et al. tried to correlate vibrational spectra of the salts with ab initio calculations [12]. However, these focused only on spectra in aqueous solu-

[*] Corresponding author. Tel.: +351-39-22826; fax: +351-39-27703; e-mail: rfausto@gemini.ci.uc.pt.

tion and the calculations were performed with a relatively modest basis set (4-31G).

In this work, FT-IR and Raman spectra of crystalline glycine salts were assigned with the help of polarized wavefunction double-ζ HF/6-31G* ab initio vibrational frequency calculations and normal coordinate analysis. All calculations were applied to the most stable conformer of each molecule studied (Fig. 1) and, since the present studies used the crystalline compounds, the cyclic dimer of the acid salt (see Fig. 1) was also considered.

The assignment of vibrational spectra was helped by extensive comparison with the spectra of zwitterionic and neutral glycine. The zwitterionic form of glycine constitutes a unique situation, because it does not correspond to a minimum in the potential energy surface of the isolated molecule [13]. The calculations were carried out using the basic molecular geometry previously determined by neutron diffraction for an individual molecule in the α-crystalline
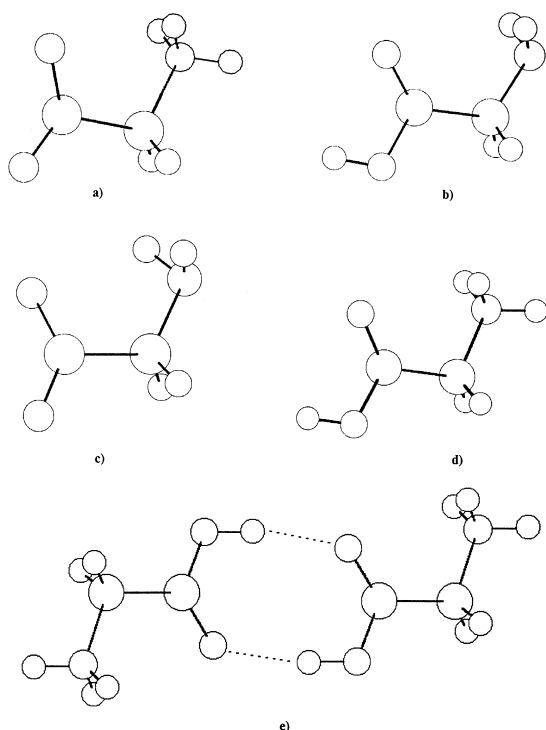

Fig. 1. Molecular structures of the various systems studied: (a) zwitterionic glycine; (b) neutral glycine; (c) glycine alkaline salt; (d) glycine acid salt (monomer) and (e) glycine acid salt (dimer).

modification of this compound [14] (glycine crystallizes in three different modifications, the α, β and γ forms [2], the α-form corresponding to the stable modification at room temperature). For zwitterionic glycine, the infrared and Raman spectra of the crystal (α-modification) were obtained, while the neutral form was studied by matrix isolation infrared spectroscopy (MI-IR), in Argon, at 10 K.

2. Experimental and computational methods

α-Glycine p.a. $+98\%$ was obtained from Merck. The alkaline salt, the glycinate ($Na^+ \cdot NH_2CH_2COO^-$), was prepared by dissolving commercial glycine p.a. in a saturated solution of NaOH. The solution (pH > 12) was dried in vacuum until complete solvent evaporation, and the crystals washed with methanol. The acid glycine salt ($^+NH_3CH_2COOH \cdot Cl^-$) was prepared by dissolution of the amino acid in concentrated HCl solution (33%) and the resulting solvent (pH < 3) was evaporated as for the alkaline salt.

Fourier transform infrared (FT-IR) spectra of crystalline materials as potassium bromide pellets were recorded with a Perkin Elmer PE 1760 FT-IR spectrometer, in the 4000–400 cm^{-1} region, with a resolution of 2 cm^{-1}.

Raman spectra were obtained using a SPEX 1403 double monochromator spectrometer (focal distance 0.85 m, aperture $f/7.8$), equipped with holographic gratings with 1800 grooves mm^{-1} (Ref. 1800-1SHD). The 514.5 nm argon laser (Spectra-Physics, model 164-05) line, adjusted to provide 220 mW power at the sample, was used as excitation radiation. Detection was effected using a thermoelectrically cooled Hamamatsu R928 photomultiplier. Spectra were recorded using increments of 1 cm^{-1} and integration times of 1 s. Under these conditions, the estimated errors in wavenumbers are ± 1 cm^{-1}.

The matrix isolation spectrum (MI-IR) of the neutral form of glycine was recorded with a dispersive Specord IR75 (updated) infrared spectrometer and a resolution of 0.2 cm^{-1}. The complete description of the set-up used for these experiments is described elsewhere [10].

Ab initio calculations were performed with a PC equipped with a Am486DX4/100 MHz processor,

using Gaussian 92 for Windows/Revision G-3 [15]. These calculations were executed at the Hartree–Fock level of theory with the 6-31G* basis set [16]. Molecular geometries were fully optimized by the force gradient method using Berny's algorithm [17]. The largest residual coordinate forces were always less than 3×10^{-4} hartree bohr^{-1} (1 hartree = 2625.5001 kJ mol^{-1}; 1 bohr = 5.29177×10^{-11} m) or hartree rad^{-1}, for bond stretches and angle bends, respectively. The stopping criterion for the SCF iterative process required a density matrix convergence of less than 10^{-8}.

The force constants (symmetry internal coordinates) used in the normal coordinate analysis were obtained from the ab initio Cartesian harmonic force constants using the program TRANSFORMER (version 2.0) [18]. This program was also used to prepare input data for the normal coordinate analysis programs: BUILD-G and VIBRAT (Refs. [19] [1] and [20]), which enabled the calculation of the potential energy distribution (PED) of each of the normal modes of vibration.

The ab initio calculated force fields were scaled down using a single scale factor (0.89), which is accepted to be the best for the Hartree–Fock level of calculations [21]. This very simple scaling preserves the potential energy distributions as they emerge from the ab initio calculation and has an important advantage over more elaborate force field scaling procedures that use more than one scale factor and usually gives rise to marked PED distortions from the ab initio calculated values.

3. Results and discussion

The optimized molecular geometries for the lowest energy conformation of the various molecules studied are shown in Table 1. The vibrational spectra of neutral and zwitterionic glycine (infrared and Raman) are shown in Figs. 2–4 and those of the alkaline and acid salts are presented in Figs. 5–8. Experimental and calculated vibrational frequencies,

intensities, their potential energy distribution and proposed assignments are presented in Tables 2–5.

In general, the assignments made for glycine (both neutral and zwitterionic form) agree with those previously proposed [2–9] and, together with the results of the calculations, were used as a basis for assignment of the spectra of the two salts. The detailed analysis and discussion of the results will be divided into sections, corresponding approximately to different spectral regions.

3.1. Region above 2000 cm^{-1}

Only neutral glycine and its acid salt contain the OH group. In the MI-IR spectrum of neutral glycine, as consequence of the isolated status in the Ar matrix, the OH stretching mode appears as a sharp band at 3560 cm^{-1}. In the infrared spectrum of the acid salt, this appears as a broad band centered at 3439 cm^{-1}. In this case, the band shape clearly shows the effect of association and hydrogen bonding. It is interesting to note that the calculated value for the frequency of this mode for a monomer in the acid salt calculations (3558 cm^{-1}; see Table 5) is considerably higher than the experimental one, while the calculated value for the dimer (3437 cm^{-1}; Table 6) is in good agreement.

Assignment of the NH and CH stretching modes in the neutral glycine infrared spectrum is straightforward, since these give rise to bands in a clear spectral region. In the alkaline salt, $\nu_{as}CH_2$ and $\nu_s CH_2$ are observed at 2945 and 2927 cm^{-1}, in the infrared spectrum and give rise to strong Raman bands at 2941 and 2911 cm^{-1}. Calculations on this molecule suggest the νNH_2 bands should appear at lower frequencies than in isolated neutral glycine (see Tables 3 and 4). Thus, these modes are assigned to the two broad medium intensity bands at 3325 cm^{-1} ($\nu_{as}NH_2$) and 3212 cm^{-1} ($\nu_s NH_2$) in the Raman spectrum of this compound. In the corresponding infrared spectrum, the νNH_2 vibrations give rise to the very broad feature from ca. 3000 to 3400 cm^{-1}. The two infrared bands at 3439 and 3391 cm^{-1} are at too high frequencies for these modes and are attributed to the first overtone of the $\nu_{as}COO^-$ stretching fundamental, which appears as a doublet at 1597 and 1561 cm^{-1}.

---

[1] These programs incorporate several routines from programs GMAT and FPERT [19].

The infrared spectra of both crystalline glycine and its acid salt show a very broad and structured band spanning from 3400 to 2400 cm^{-1}. This is typical of crystalline amino acids [5,22] and has been ascribed to NH_3 stretching modes, which sometimes obscure the CH_2 stretching bands. In the Raman spectra, the νCH_2 modes increase and the νNH_3 modes decrease in intensity, which allows a clear observation of the first. The origin of the extensive broadening and complex structure of the νNH_3 stretching region in the infrared spectrum of crystalline amino acids has been extensively discussed [5,23–26]. Although still controversial, it is generally considered that the observed band contour results essentially from Fermi resonance between the νNH_3 stretching modes and combination bands involving mainly the δNH_3 bending vibrations [5]. This interpretation is reinforced by the present results. Al-

Table 1
Calculated (ab initio 6-31G*) optimized molecular geometries[a]

Coordinate	Glycine (neutral form)	Glycine[b] (zwitterion)	Alkaline salt	Acid salt (monomer)	Acid salt (dimer)
C=O	1.188	1.233	1.233	1.184	1.197
C–C	1.515	1.553	1.553	1.517	1.515
C–O	1.330	1.237	1.237	1.301	1.289
C–N	1.439	1.496	1.463	1.496	1.495
O–H	0.952			0.957	0.964
C–H	1.085	1.080	1.086	1.080	1.081
	1.085	1.080	1.089	1.080	1.081
N–H$_{op}$	1.002	1.012	1.005	1.012	1.013
	1.002	1.012	1.005	1.012	1.013
N–H$_{ip}$		1.011		1.011	1.013
H...O=					1.948
C–C–O	111.8	117.5	115.6	111.4	111.6
C–C=O	125.4	117.1	116.7	120.8	121.1
O=C–O	122.8	125.4	129.7	127.8	127.2
N–C–C	115.0	111.9	115.7	106.8	108.6
C–O–H	108.4			111.3	112.4
C–C–H	107.7	108.8	109.0	111.4	110.7
	107.7	110.5	107.4	111.4	110.7
C–N–H$_{op}$	110.4	110.4	104.6	110.9	111.6
	110.4	111.7	106.9	110.9	111.6
C–N–H$_{ip}$		112.1		112.2	111.5
O–H...O=					170.3
C=O...H					130.1
C–C(=O)–O	180.0	180.0	178.2	180.0	180.0
N–C–C=O	0.0	18.9	11.8	0.0	0.0
O=C–O–H	0.0			0.0	0.0
H–C–C=O	−123.0	−101.0	−107.9	−118.8	−119.5
	123.0	140.6	133.7	118.8	119.5
H$_{op}$–N–C–C	−58.6	−58.1	−37.7	−58.5	−59.3
H$_{ip}$–N–C–C		−177.3		180.0	180.0

[a]Bond lengths in Å, angles in degrees; geometries refer to the most stable conformer in the RHF/6-31G* PES of each molecule studied.
[b]Zwitterionic form of glycine does not correspond to a minimum in the PES of this molecule [13]. The geometry here presented and used to undertake the vibrational calculations was built as follows: (i) valence angles and dihedrals were taken from the neutron diffraction data relative to crystalline glycine (α-form) [14]; (ii) bond lengths were transferred from the 6-31G* optimized structures here calculated for the alkaline salt (COO$^-$ group) and acid salt (NH$_3^+$ group). The calculated bond lengths obtained for the two salts were used instead of the experimental data obtained from neutron diffraction since otherwise it would not be possible to adopt the single force field scaling factor used in this study to fit the calculated frequencies to the experimental spectra also for the zwitterionic form of glycine. Indeed, the scale factor requires 6-31G* consistent data, in particular in the case of bond lengths, whose particular values strongly influence the calculated frequencies.
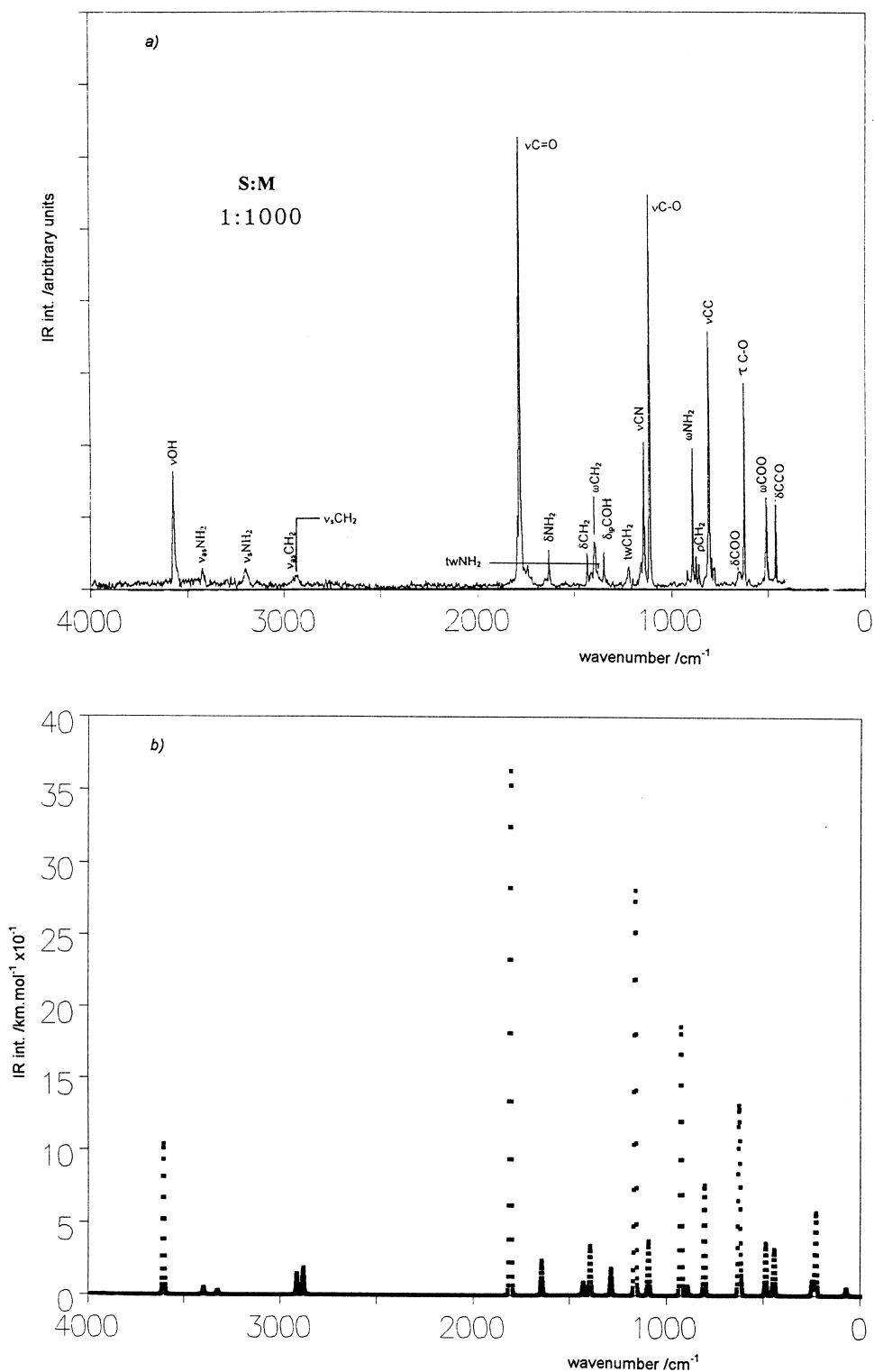
Fig. 2. Infrared spectra of neutral form of glycine: (a) experimental (MI-IR spectrum of glycine isolated in an Ar matrix at 10 K) and (b) 6-31G* predicted infrared spectrum (scaled).
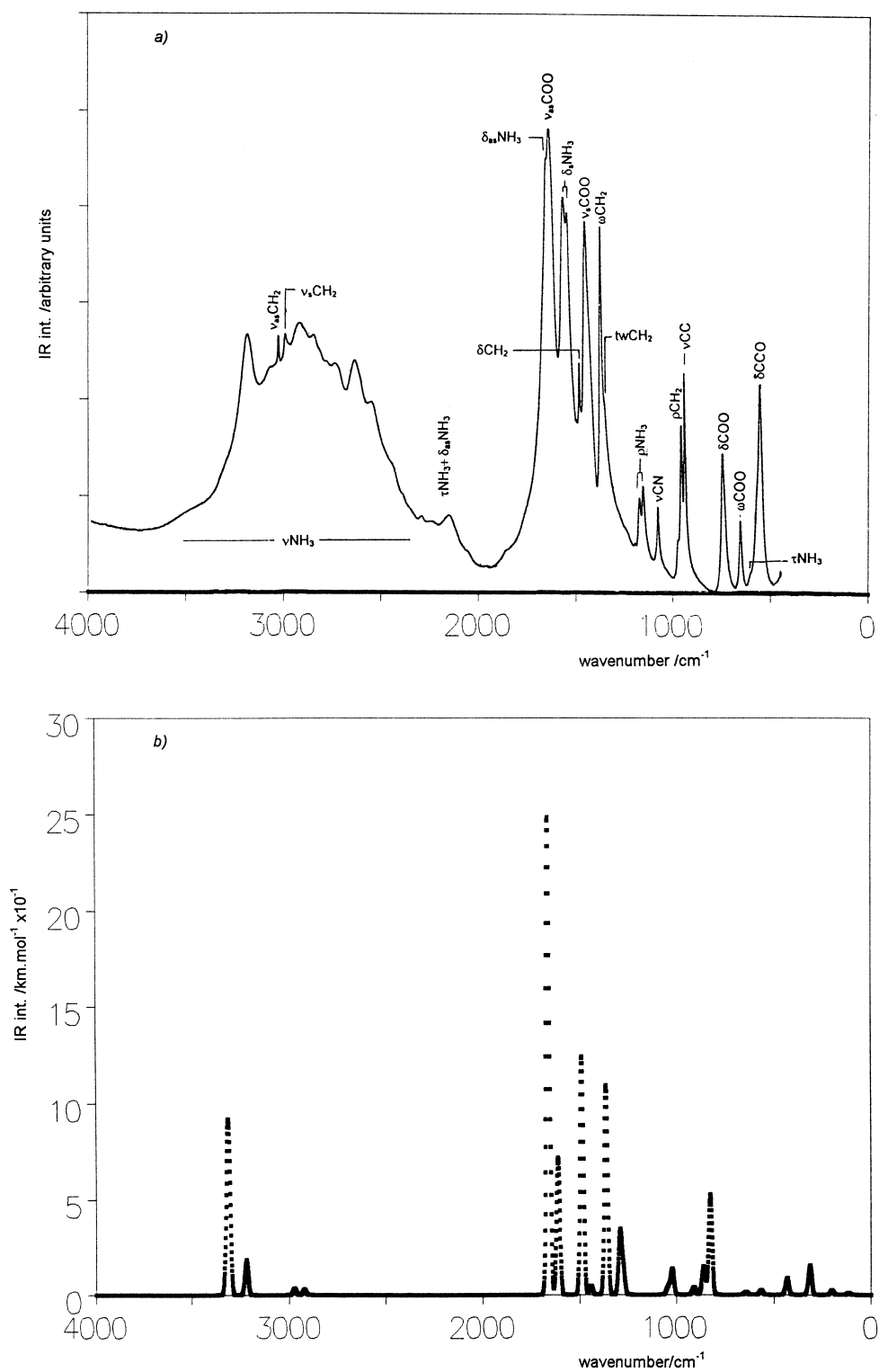
Fig. 3. Infrared spectra of zwitterionic glycine: (a) experimental (FT-IR spectrum of crystalline glycine at room temperature) and (b) 6-31G * predicted infrared spectrum (scaled).
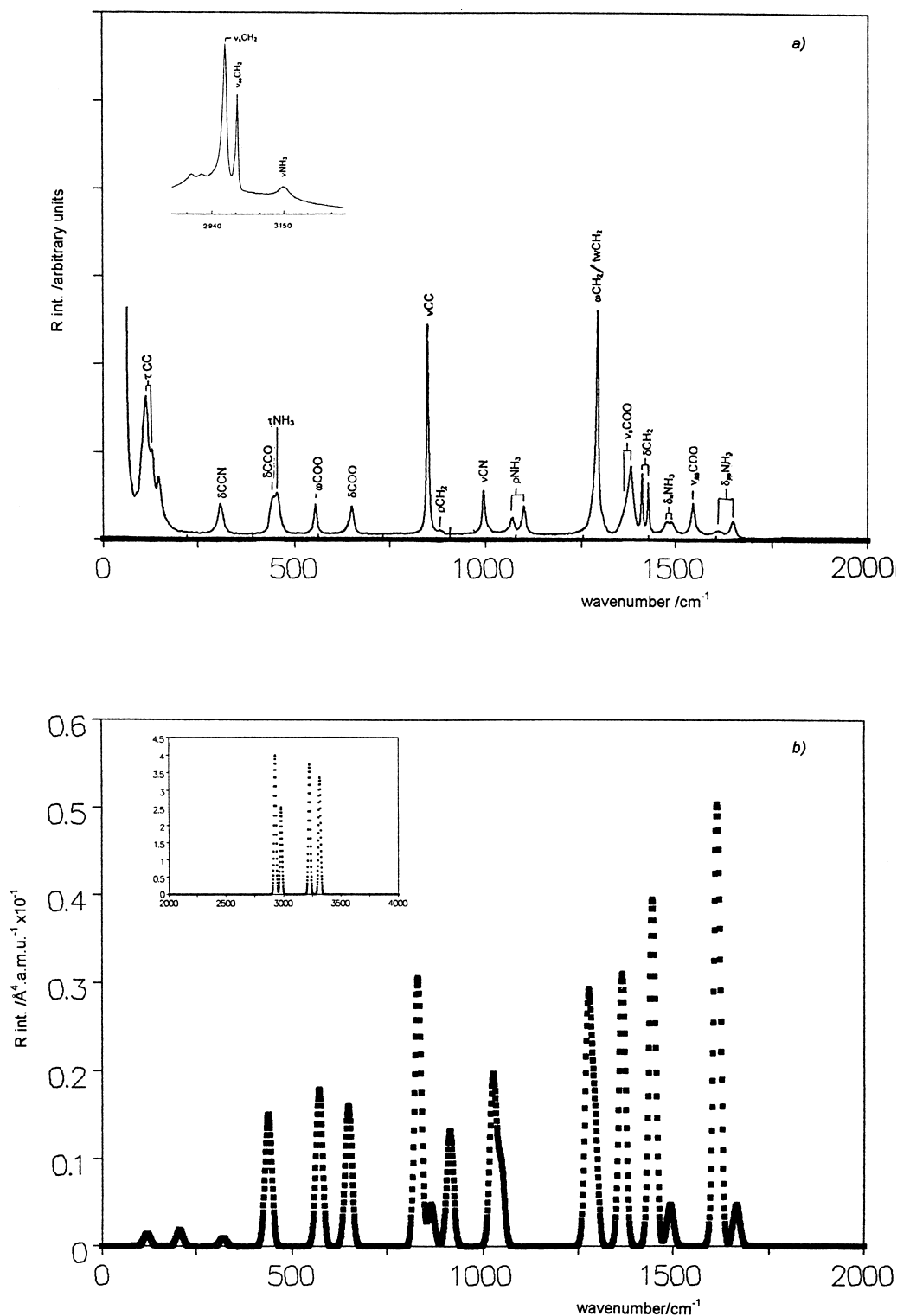
Fig. 4. Raman spectra of zwitterionic glycine: (a) experimental (Raman spectrum of crystalline glycine at room temperature) and (b) 6-31G * predicted Raman spectrum (scaled).
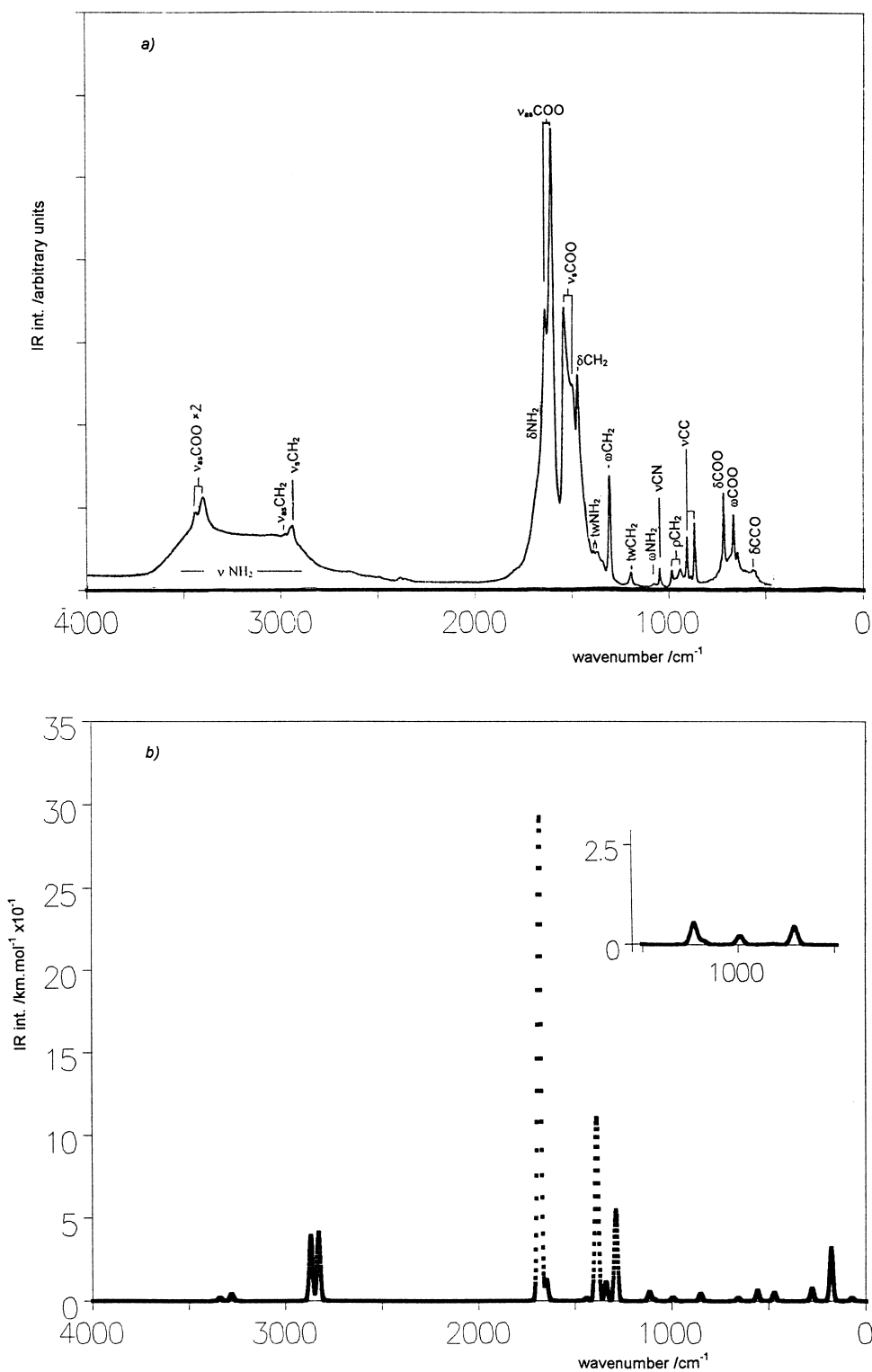
Fig. 5. Infrared spectra of glycine alkaline salt: (a) experimental (FT-IR spectrum of crystalline $Na^+ \cdot NH_2CH_2COO^-$ at room temperature) and (b) 6-31G* predicted infrared spectrum (scaled).
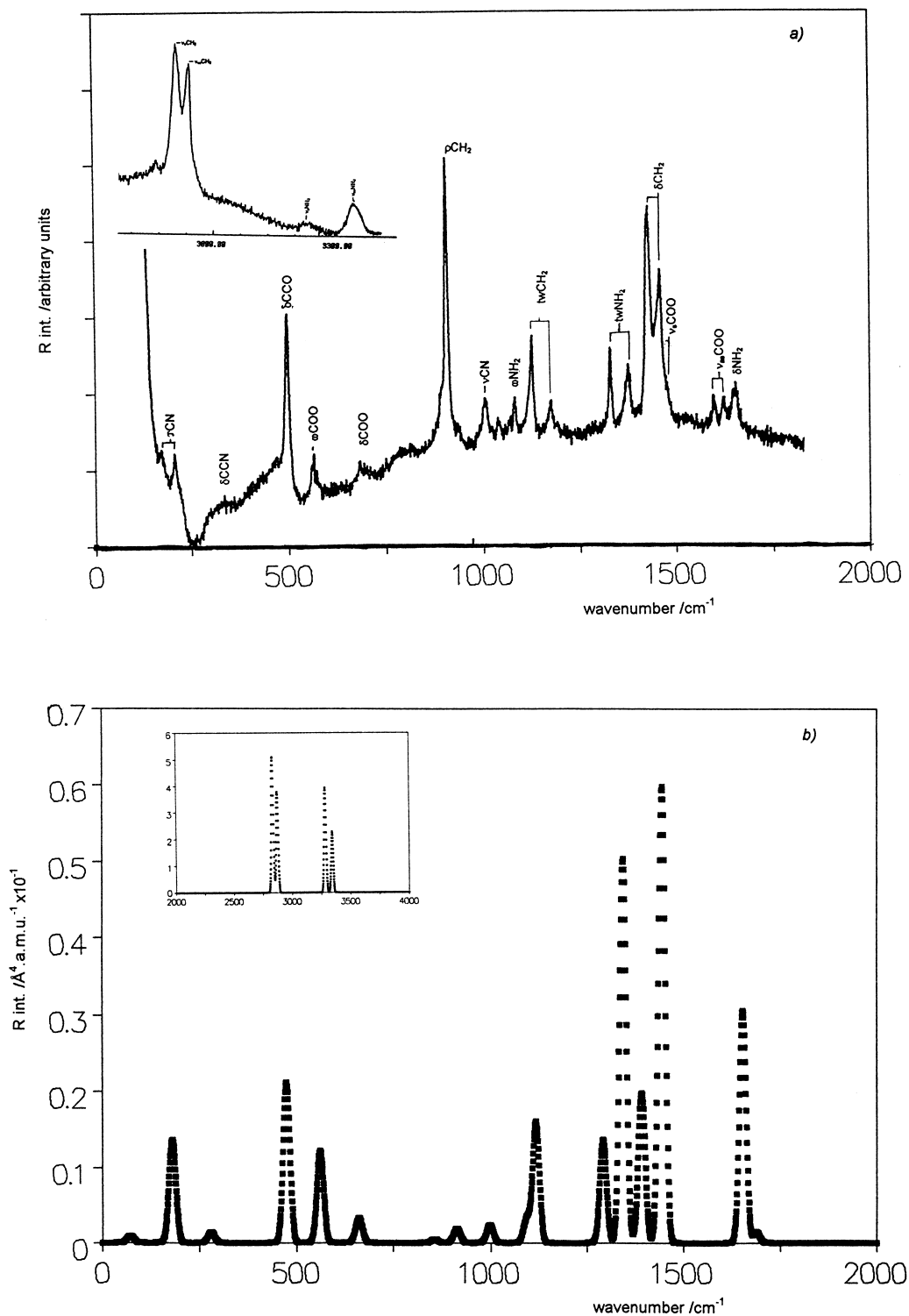
Fig. 6. Raman spectra of glycine alkaline salt: (a) experimental (Raman spectrum of crystalline $Na^+ \cdot NH_2CH_2COO^-$ at room temperature) and (b) 6-31G* predicted Raman spectrum (scaled).
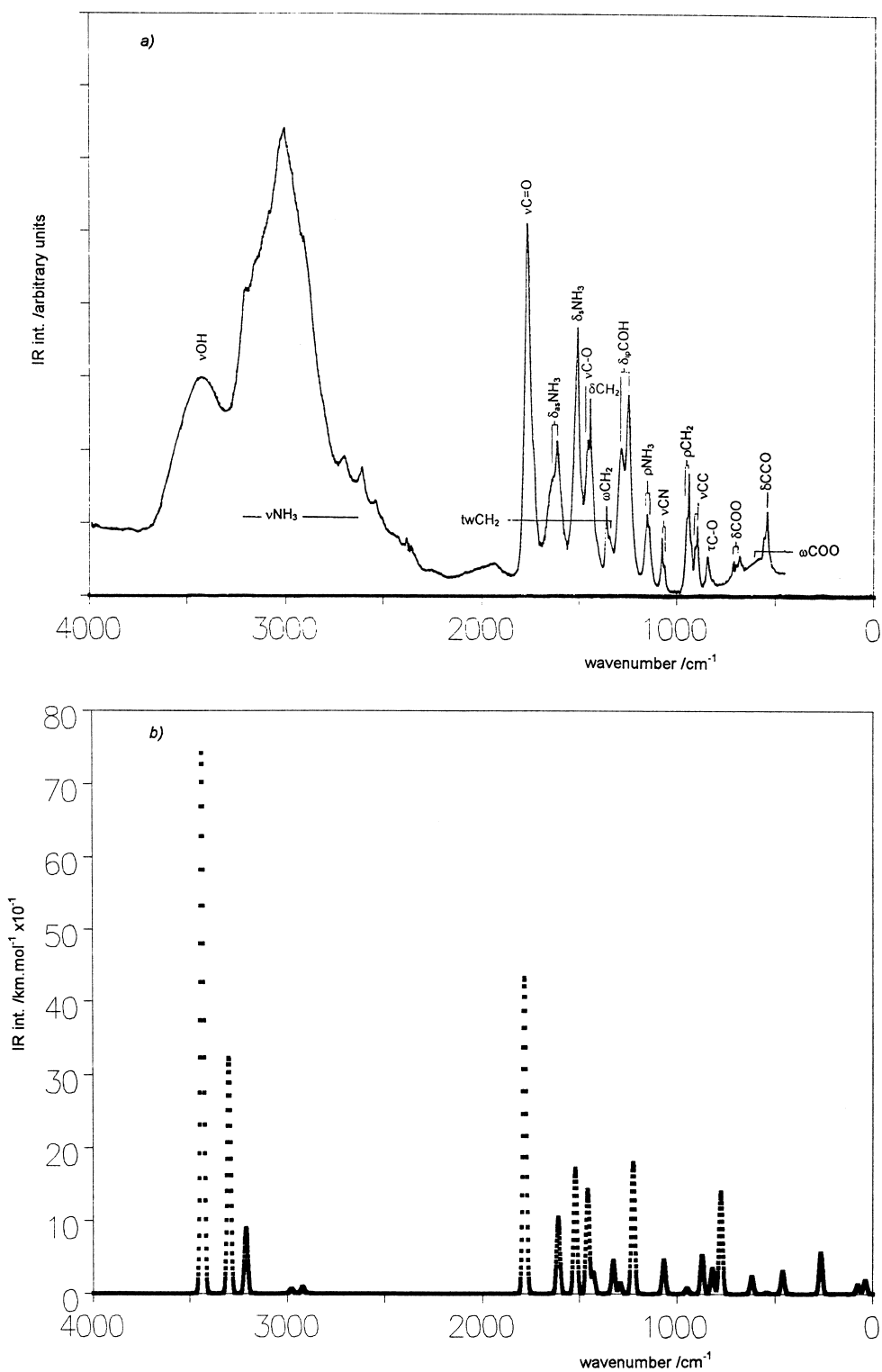
Fig. 7. Infrared spectra of glycine acid salt: (a) experimental (FT-IR spectrum of crystalline $^{+}NH_3CH_2COOH \cdot Cl^{-}$ at room temperature) and (b) 6-31G* predicted infrared spectrum (dimer 'model'; scaled).

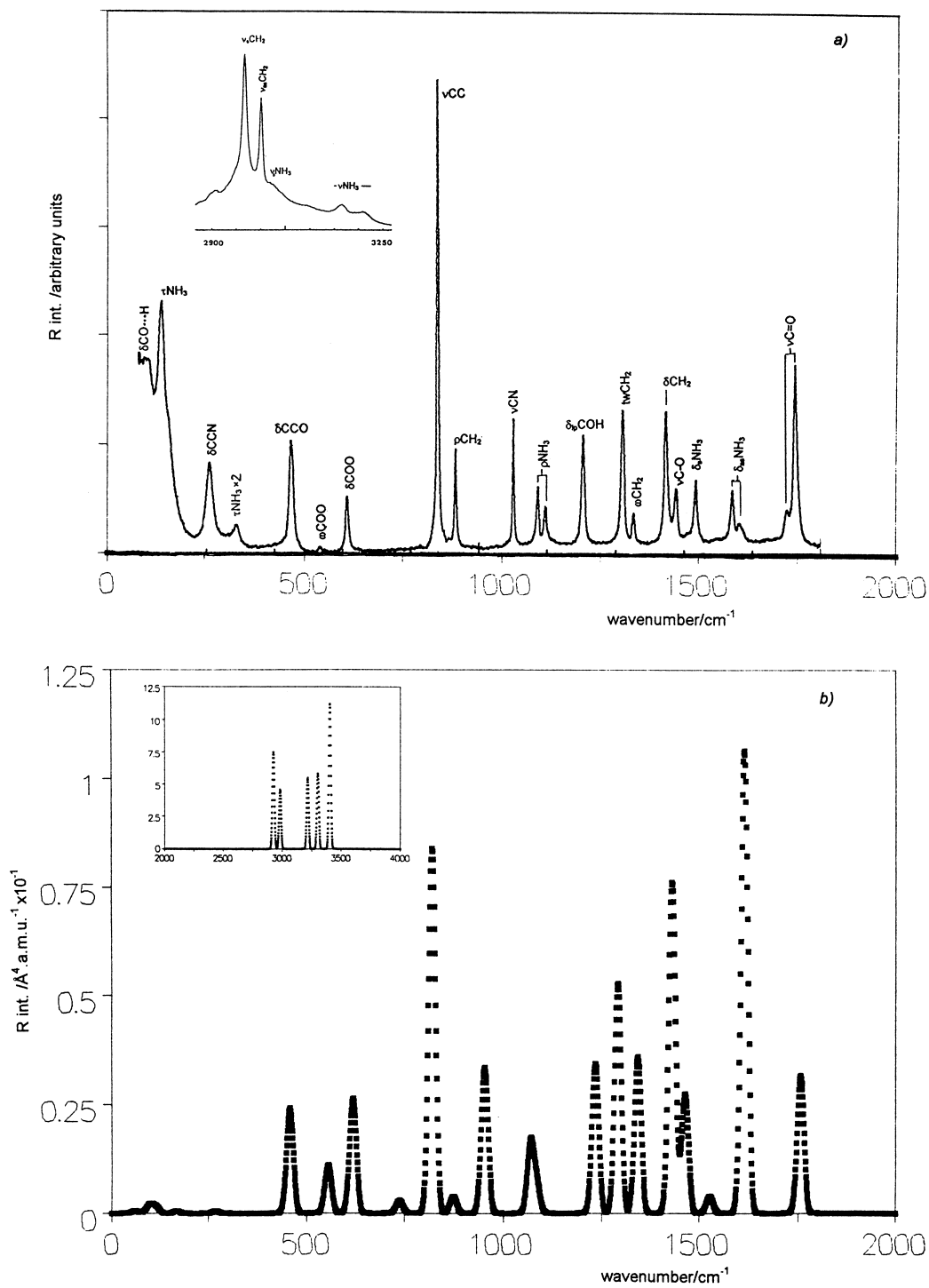Fig. 8. Raman spectra of glycine alkaline salt: (a) experimental (Raman spectrum of crystalline $^{+}NH_3CH_2COOH \cdot Cl^{-}$ at room temperature) and (b) 6-31G* predicted Raman spectrum (dimer 'model'; scaled).

Table 2
Spectra assignment and potential energy distribution for the zwitterionic form of glycine[a]

Assignment	Symmetry	Calculated			Experimental (IR)		Experimental (Raman)		
		Wavenumber	IR int.	R int.	Wavenumber	Intensity	Wavenumber	Intensity	P.E.D.
$\nu_{as}NH_3$	A	3319	131.0	27.8	3176, 3040	s, s	3149	m	$\nu'_{as}NH_3$
$\nu_{as}NH_3$	A	3311	86.0	51.5	3176, 3040	s, s	3149	m	$\nu''_{as}NH_3$
$\nu_s NH_3$	A	3224	38.9	79.5	2899[b]	w	2911,2886	m, m	$\nu_s NH_3$
$\nu_{as}CH_2$	A	2977	7.3	53.6	3007	w	3013	s	$\nu_{as}CH_2$
$\nu_s CH_2$	A	2926	6.1	84.9	2970	vs	2978	s	$\nu_s CH_2$
$\nu_{as}COO$	A	1666	528.5	1.0	1596	vs	1575	w	$\nu_{as}COO$ (83), $\delta'_{as}NH_3$ (10)
$\delta_{as}NH_3$	A	1616	109.0	5.5	1615	s	1676,1638	w, vw	$\delta'_{as}NH_3$ (40), $\delta''_{as}NH_3$ (40), $\nu_{as}COO$ (10)
$\delta_{as}NH_3$	A	1614	44.3	5.3	1615	s	1676,1638	w, vw	$\delta''_{as}NH_3$ (47), $\delta'_{as}NH_3$ (42)
$\delta_s NH_3$	A	1493	264.2	1.0	1525,1505	s, s	1522,1511	w, w	$\delta_s NH_3$
δCH_2	A	1446	9.7	8.4	1460,1444	vw, m	1462, 1446	m, m	δCH_2
$\nu_s COO$	A	1367	232.5	6.6	1413,1401	s, m	1417,1404	m, sh	$\nu_s COO$ (72), νCC (20), δCOO (15), ωCH_2 (14)
ωCH_2	A	1294	69.6	2.8	1334	s	1331	s	ωCH_2 (59), $\nu_s COO$ (22)
$twCH_2$	A	1277	26.6	5.8	1310	w	1331	s	$twCH_2$ (46), $\rho''NH_3$ (18)
ρNH_3	A	1046	8.6	1.9	1131	w	1144	w	$\rho'NH_3$ (29), $twCH_2$ (21), ρNH_3 (16), ωCOO (15), ρCH_2 (11)
ρNH_3	A	1025	28.3	4.1	1112	w	1114	w	$\rho''NH_3$ (32), $twCH_2$ (19), $\rho'NH_3$ (16), ρCH_2 (11), ωCH_2 (11)
νCN	A	914	8.3	2.8	1034	w	1041	w	νCN (69), νCC (19)
ρCH_2	A	865	31.6	1.0	911	m	928	vw	ρCH_2 (28), $\rho''NH_3$ (47), ωCOO (28)
νCC	A	831	111.9	6.5	893	m	899	s	νCC (76), νCN (19)
δCOO	A	648	3.0	3.4	698	m	703	w	δCOO (61), ρCH_2 (19), νCC (11)
ωCOO	A	571	5.0	3.8	608	w	608	w	ωCOO (43), ρCH_2 (24), νCC (19), δCOO (16)
δCCO	A	437	18.5	3.2	504	m	499	w	δCCO (44), νCC (14)
δNCC	A	320	32.7	0.2	358[c]		364	w	δNCC (66), δCCO (45)
τCN	A	206	4.8	0.4	520[d]	sh	509[d]	w	τCN
τCC	A	119	2.1	0.3			186,171	w, m	τCC (46), τCN (22), ωCOO (13)

[a] Wavenumber values are in cm^{-1}. IR int. (infrared intensities) $km \cdot mol^{-1}$ and R int. (Raman scattering activities) in $Å^4/amu$. ν stretching, δ bending, ω wagging, ρ rocking, tw twisting, τ torsion, s symmetric, as asymmetric. The experimental intensities are only qualitative. PED: The number is parenthesis is the percent contribution of each internal mode for the total potential energy. Contributions < 10% are not shown. When only one internal mode in the PED have a contribution > 10%, its value is ommited.

[b] Higher component band of the complex structured band due to Fermi resonance interaction; other main relative maxima occur at 2830, 2733, 2622 and 2532 cm^{-1} (see text).

[c] The predicted wavenumber for τCN is considerably lower than the experimental value, due to crystal packing forces (see text).

[d] From Ref. [9].

Table 3

Spectra assignment and potential energy distribution for the neutral form of glycine[a]

Assignment	Symmetry	Calculated		Experimental (MI-IR)		
		Wavenumber	IR int.	Wavenumber	Intensity	P.E.D.
νOH	A'	3607	110.1	3560	m	νOH
$\nu_{as} NH_2$	A''	3400	5.0	3410	w	$\nu_{as} NH_2$
$\nu_s NH_2$	A'	3328	3.0	3200	w	$\nu_s NH_2$
$\nu_{as} CH_2$	A''	2915	15.5	2957	w	$\nu_{as} CH_2$
$\nu_s CH_2$	A'	2881	19.9	2943	w	$\nu_s CH_2$
$\nu C=O$	A'	1811	385.9	1780	vs	$\nu C=O$
δNH_2	A'	1648	25.4	1630, 1623	w	δNH_2 (71), ωNH_2 (24)
δCH_2	A'	1433	9.2	1428	w	δCH_2
ωCH_2	A'	1397	36.4	1385	w	ωCH_2 (48), νCC (16), $\nu C–O$ (15)
$tw NH_2$	A''	1349	0.0	1373	vw	$tw NH_2$ (47), $tw CH_2$ (47)
δCOH	A'	1288	19.4	1339	w	δCOH (38), ωCH_2 (33), $\nu C–O$ (10)
$\nu C–O$	A'	1165	299.0	1100	s	$\nu C–O$ (43), δCOH (34)
$tw CH_2$	A''	1154	2.1	1147	w	$tw CH_2$ (49), $tw NH_2$ (32), ρCH_2 (11)
νCN	A'	1096	39.9	1131	m	νCN
ωNH_2	A'	930	198.2	882, 880	m, w	ωNH_2 (46), νCN (17), δNH_2 (16)
ρCH_2	A''	897	6.6	867, 852	w, w	ρCH_2 (43), $tw NH_2$ (26), ωCOO (21)
νCC	A''	809	80.3	799	s	νCC (46), ωNH_2 (13)
$\tau C–O$	A''	630	137.9	618	m	$\tau C–O$ (50), ωCOO (30), ρCH_2 (17)
δCOO	A'	621	15.7	637	w	δCOO (50), δNCC (16), $\delta CC=O$ (12), $\nu C–O$ (10)
ωCOO	A''	491	38.6	498	w	ωCOO (37), $\tau C–O$ (40), ρCH_2 (17)
$\delta CC=O$	A'	448	34.1	463	m	$\delta CC=O$ (27), δCOO (34), νCC (15), δNCC (11)
δNCC	A'	250	10.8			δNCC (47), $\delta CC=O$ (47)
τCN	A''	232	60.3			τCN
τCC	A''	74	5.2			τCC (69), τCN (13)

[a] Wavenumber values are in cm^{-1}. IR int. (infrared intensities) $km \cdot mol^{-1}$. ν, stretching; δ, bending; ω, wagging; ρ, rocking; tw, twisting; τ, torsion; s, symmetric; as, asymmetric. The experimental intensities are only qualitative. PED: The number is parenthesis is the percent contribution of each internal mode for the total potential energy. Contributions < 10% are not shown. When only one internal mode in the PED have a contribution > 10%, its value is ommited.

though more elaborate studies on this problem are still required, our data are consonant with the following assignments:

(i) The infrared bands at 3176 and 3040 cm^{-1} (with the first also present in the infrared spectrum of crystalline ND_3 deuterated zwitterionic glycine [5]) are mainly due to $\nu_{as} NH_3$ in Fermi resonance with the first overtone of the $\nu_{as} COO^-$ mode (fundamental: 1596 cm^{-1}). The doublet of bands at 3209 and 3165 cm^{-1} in the Raman spectrum of glycine acid salt has a similar origin (in the infrared spectrum of this compound only the lower frequency component can be observed, since the higher component band is buried within the more intense very broad νOH stretch band). This interpretation is reinforced by the observation in the infrared spectrum of crystalline ND_3 deuterated zwitterionic glycine of a

band at 3113 cm^{-1}, due to the first overtone of the $\nu_{as} COO^-$ stretching, whose fundamental occurs at 1592 cm^{-1} [6].

(ii) In the Raman spectrum of crystalline glycine, the $\nu_{as} NH_3$ modes give rise to a single broad band with maximum intensity at ca. 3149 cm^{-1} (close to the average frequency of the doublet of bands observed in the corresponding infrared spectrum).

(iii) The $\nu_s NH_3$ stretching is extensively involved in Fermi resonance with combination bands. For zwitterionic glycine, we tentatively interpret the maxima at 2899, 2830, 2732, 2622 and 2532 cm^{-1} to bands resulting mainly from Fermi interaction with $\delta_s NH_3 + \nu_s COO^-$ (1505 + 1413 cm^{-1}), $\delta_s NH_3 + \omega CH_2$ (1505 + 1334 cm^{-1}), $\delta_{as} NH_3 + \rho NH_3$ (1615 + 1112 cm^{-1}), $\delta_{as} NH_3 + \nu CN$ (1615 + 1034 cm^{-1}) and $\delta_{as} NH_3 + \rho CH_2$ (1615 + 911

Table 4

Spectra assignment and potential energy distribution for the glycine alkaline salt[a]

Assignment	Symmetry	Calculated			Experimental (IR)		Experimental (Raman)		P.E.D.
		Wavenumber	IR int.	R int.	Wavenumber	Intensity	Wavenumber	Intensity	
$\nu_{as}NH_2$	A	3342	4.1	48.4			3325	m	$\nu_{as}NH_2$
$\nu_s NH_2$	A	3282	8.9	83.6			3212	m	$\nu_s NH_2$
$\nu_{as}CH_2$	A	2872	82.5	80.3	2945	m	2941	vs	$\nu_{as}CH_2$ (80), $\nu_s CH_2$ (19)
$\nu_s CH_2$	A	2831	87.2	108.7	2927	m	2911	vs	$\nu_s CH_2$ (80), $\nu_{as}CH_2$ (20)
$\nu_{as}COO$	A	1688	622.3	0.3	1597, 1561	s, vs	1597,1572	w, w	$\nu_{as}COO$
δNH_2	A	1652	26.4	6.5	1630	sh	1630	w	δNH_2
δCH_2	A	1444	3.3	12.7	1431	m	1439,1410	s, s	δCH_2
$\nu_s COO$	A	1392	234.3	4.2	1498, 1457	s, m	1462	sh	$\nu_s COO$ (56), νCC (18), δCOO (14)
$twNH_2$	A	1344	23.7	10.7	1355, 1336	w, w	1358,1314	m, m	$twNH_2$ (53), $twCH_2$ (33)
ωCH_2	A	1292	115.1	2.9	1270	m			ωCH_2 (70), $\nu_s COO$ (12)
$twCH_2$	A	1118	11.5	3.4	1159	w	1168,1122	w, m	$twCH_2$ (48), $twNH_2$ (23)
ωNH_2	A	1094	2.0	0.7	1069	w	1079	w	ωNH_2 (47), νCN (17)
νCN	A	997	4.6	0.5	1009	w	1004	w	νCN (54), ωNH_2 (28)
ρCH_2	A	912	0.4	0.4	944, 900	w, w	909	vs	ρCH_2 (39), $twNH_2$ (25), ωCOO (25)
νCC	A	855	9.6	0.1	865, 827	w			νCC (37), δCOO (33), $\nu_s COO$ (12)
δCOO	A	661	3.9	0.7	674	w	636	w	δCOO (36), δNCC (21), νCC (12), δCCO (10)
ωCOO	A	561	13.5	2.6	622	m	582	w	ωCOO (49), ρCH_2 (30)
δCCO	A	474	10.9	4.5	519	w	517	s	δCCO (41), νCC (18), δNCC (11)
δNCC	A	280	16.1	0.3			261	w	δNCC (54), δCCO (38)
τCN	A	180	67.9	2.9			239, 206	m, sh	τCN
τCC	A	73	3.9	0.2					τCC (63), τCN (12)

[a]Wavenumber values are in cm^{-1}. IR int. (infrared intensities) km·mol^{-1} and R int. (Raman scattering activities) in Å^4/amu. ν, stretching; δ, bending; ω, wagging; ρ, rocking; tw, twisting; τ, torsion; s, symmetric; as, asymmetric. The experimental intensities are only qualitative. PED: The number in parentheses is the percent contribution of each internal mode for the total potential energy. Contributions < 10% are not shown. When only one internal mode in the PED has a contribution > 10%, its value is ommited.

Table 5
Calculated spectra and potential energy distribution for the glycine acid salt (monomer 'model')[a]

Assignment	Symmetry	Wavenumber	IR int.	R int.	P.E.D.
νOH	A'	3558	244.9	69.4	νOH
ν_{as}NH$_3$	A'	3320	155.3	37.9	ν_{as}NH$_3$
ν_{as}NH$_3$	A''	3303	167.5	23.7	ν_{as}NH$_3$
ν_sNH$_3$	A'	3223	77.2	54.8	ν_sNH$_3$
ν_{as}CH$_2$	A''	2988	2.9	47.8	ν_{as}CH$_2$
ν_sCH$_2$	A'	2929	3.9	79.0	ν_sCH$_2$
νC=O	A'	1825	414.7	5.1	νC=O
δ_{as}NH$_3$	A'	1614	44.6	4.9	δ_{as}NH$_3$
δ_{as}NH$_3$	A''	1608	65.0	6.1	δ_{as}NH$_3$
δ_sNH$_3$	A'	1521	187.8	0.5	δ_sNH$_3$
νC–O	A'	1440	106.7	4.3	νC–O (15), δCH$_2$ (38), νCC (18), ωCH$_2$ (16)
δCH$_2$	A'	1435	41.3	4.3	δCH$_2$ (53), ωCH$_2$ (21)
ωCH$_2$	A'	1311	42.3	1.5	ωCH$_2$ (46), δCOH (18), νC–O (17)
twCH$_2$	A''	1286	17.3	5.6	twCH$_2$ (67), ρNH$_3$ (21)
δCOH	A'	1181	234.3	3.3	δCOH (54), νC–O (32)
ρNH$_3$	A''	1078	0.2	1.0	ρNH$_3$ (29), twCH$_2$ (33), ρCH$_2$ (23), ωCOO (12)
ρNH$_3$	A'	1065	43.0	1.7	ρNH$_3$ (59), ωCH$_2$ (15)
νCN	A'	939	8.2	3.5	νCN (74), νCC (13)
ρCH$_2$	A''	873	40.5	0.4	ρCH$_2$ (33), ρNH$_3$ (42), ωCOO(15)
νCC	A'	807	45.4	9.9	νCC (44), νCN (11), ρNH$_3$(11)
τC–O	A''	632	143.6	0.3	τC–O (67), ωCOO (22)
δCOO	A'	608	25.7	2.9	δCOO (50), δNCC (16), δCC=O (12)
ωCOO	A''	509	44.9	2.7	ωCOO (58), ρCH$_2$ (23)
δCC=O	A'	448	57.1	1.5	δCC=O (29), δCOO (29), δNCC (14)
δNCC	A'	265	25.7	0.1	δNCC (48), δCC=O (47)
τCN	A''	161	0.9	0.0	τCN (65), τCC (22)
τCC	A''	48	5.3	0.1	τCC (44), τCN (38)

[a]Wavenumber values are in cm^{-1}. IR int. (infrared intensities) km·mol^{-1} and R int. (Raman scattering activities) in Å^4/amu. ν, stretching; δ, bending; ω, wagging; ρ, rocking; tw, twisting; τ, torsion; s, symmetric; as, asymmetric. P.E.D.: The number in parentheses is the percent contribution of each internal mode for the total potential energy. Contributions < 10% are not shown. When only one internal mode in the PED has a contribution > 10%, its value is ommited.

cm^{-1}). In the acid salt, the corresponding bands appear at 3003, 2840, 2678, 2595 and 2525 cm^{-1}, with the dominant band at 3003 cm^{-1}.

(iv) The frequencies of the νNH$_2$ stretching modes in the alkaline salt of glycine and, in particular, the νNH$_3$ vibrations in both crystalline glycine and its acid salt are considerably overestimated by the calculations, since these groups participate in intermolecular hydrogen bonding that is not properly considered in the calculations. However, the calculations are able to predict correctly the general trends, both with respect to relative positions of the various νNH vibrations within the same molecule and the relative values for the same mode in different molecules (see Tables 2–6).

In the infrared spectrum of the crystalline glycine, in addition to the bands due to the νNH$_3$ and νCH$_2$

stretching modes, a band of medium intensity is also observed at 2117 cm^{-1}, and is here assigned to the combination mode δ_{as}NH$_3$ + τNH$_3$. As discussed in Section 3.2 the fundamentals are assigned to the bands at 1615 and 520 cm^{-1}.

3.2. Region 2000–1400 cm^{-1}

This region of the spectrum includes the carbonyl stretching band (νC=O), NH$_2$ and NH$_3$ bending modes, CH$_2$ scissoring and the two carboxylate stretching modes (ν_{as}COO$^-$ and ν_sCOO$^-$).

The carbonyl stretching band is present in both neutral glycine and acid salt spectra and can be assigned to the intense infrared bands at 1780 cm^{-1} (glycine) and 1745 cm^{-1} (acid salt; B_u mode) and to the doublet of bands at 1737 and 1717 cm^{-1} in the

Table 6
Spectra assignment and potential energy distribution for the glycine acid salt dimer[a]

Assignment	Symmmetry	Calculated			Experimental (IR)		Experimental (Raman)		P.E.D.
		Wavenumber	IR int.	R int.	Wavenumber	Intensity	Wavenumber	Intensity	
νOH	B_u	3437	1590.0		3439	vs			νOH
νOH	A_g	3404		238.8					νOH
ν_{as}NH$_3$	A_g	3303		78.2			3209, 3165	m, m	ν_{as}NH$_3$
ν_{as}NH$_3$	B_u	3302	353.5		3196	s			ν_{as}NH$_3$
ν_{as}NH$_3$	A_u	3302	333.4		3196	s			ν_{as}NH$_3$
ν_{as}NH$_3$	B_g	3302		45.7			3209, 3165	m, m	ν_{as}NH$_3$
ν_sNH$_3$	A_g	3216		116.4			3020	m	ν_sNH$_3$
ν_sNH$_3$	B_u	3216	189.1		3003	vs			ν_sNH$_3$
ν_{as}CH$_2$	A_u	2982	13.2						ν_{as}CH$_2$
ν_{as}CH$_2$	B_g	2982		97.2			3001	vs	ν_{as}CH$_2$
ν_sCH$_2$	A_g	2925		159.1			2968	vs	ν_sCH$_2$
ν_sCH$_2$	B_u	2925	19.0						ν_sCH$_2$
νC=O	B_u	1787	919.2		1745	vs			νC=O (89), νC–O (14)
νC=O	A_g	1756		6.7			1737, 1717	m, w	νC=O (90), νC–O (11)
δ_{as}NH$_3$	A_g	1614		9.6			1601	w	δ_{as}NH$_3$
δ_{as}NH$_3$	B_u	1614	84.5		1625	m			δ_{as}NH$_3$
δ_{as}NH$_3$	A_u	1612	137.6		1594	m			δ_{as}NH$_3$
δ_{as}NH$_3$	B_g	1612		13.2			1585	m	δ_{as}NH$_3$
δ_sNH$_3$	A_g	1526		0.8			1494	m	δ_sNH$_3$
δ_sNH$_3$	B_u	1525	363.4		1486	s			δ_sNH$_3$
νC–O	A_g	1464		5.8			1445	w	νC–O (32), ωCH$_2$ (26), νCC (21), δCOO (12)
νC–O	B_u	1461	301.0		1437	s			νC–O (29), ωCH$_2$ (30), νCC (24), δCOO (12)
δCH$_2$	A_g	1431		16.2			1421	m	δCH$_2$
δCH$_2$	B_u	1431	60.6		1421	s			δCH$_2$
ωCH$_2$	A_g	1344		7.6			1342	w	ωCH$_2$ (53), δCOH (23)
ωCH$_2$	B_u	1328	96.4		1332	m			ωCH$_2$ (52), δCOH (21), νC–O (14)
twCH$_2$	A_u	1292	31.1		1313	w			twCH$_2$ (60), ρNH$_3$ (17)
twCH$_2$	B_g	1292		11.2			1315	m	twCH$_2$ (60), ρNH$_3$ (17)
δCOH	A_g	1234		7.3			1219	m	δCOH (46), νC–O (40)
δCOH	B_u	1226	380.9		1254, 1216	s, s			δCOH (64), νC–O (31)
ρNH$_3$	A_u	1085	0.6		1115	w			ρNH$_3$ (34), twCH$_2$ (32), ρCH2 (26), ωCOO (14)
ρNH$_3$	B_g	1085		1.3			1125	w	ρNH$_3$ (34), twCH$_2$ (32), ρCH2 (26), ωCOO (14)

		Calc.	Int.	Exp. (IR)		Exp. (R)		PED
ρNH_3	A_g	1069	3.4			1108	m	ρNH_3 (65), ωCH_2 (15)
ρNH_3	B_u	1069	98.3	1103	m			ρNH_3 (65), ωCH_2 (14)
νCN	A_g	952	7.1			1047	m	νCN (72), νCC (15)
νCN	B_u	951	16.3	1040, 1027	w, w			νCN (72), νCC (14)
ρCH_2	A_u	875	111.9	912, 900	sh, m			ρCH_2 (35), ρNH_3 (45), ωCOO (20)
ρCH_2	B_g	873	0.8			904	m	ρCH_2 (36), ρNH_3 (46), ωCOO (20)
νCC	B_u	823	73.8	870, 857	w, w			νCC (42), νCN (15), δCOO (14), ρNH_3 (12)
νCC	A_g	819	17.8			860	vs	νCC (44), νCN (15), δCOO (13), ρNH_3 (12)
$\tau C–O$	A_u	780	295.3	804	w			$\tau C–O$ (73), δ_{op}(ring) (12)
$\tau C–O$	B_g	737	0.6					$\tau C–O$ (90)
δCOO	B_u	622	50.6	675, 640	w, w			δCOO (48), δNCC (15), $\delta CC=O$ (11)
δCOO	A_g	618	5.6			637	m	δCOO (51), δNCC (14), $\delta CC=O$ (10)
ωCOO	B_g	555	2.3			571	w	ωCOO (63), ρCH_2 (23)
ωCOO	A_u	545	3.9	≈ 540	vw			ωCOO (61), ρCH_2 (23)
$\delta CC=O$	B_u	464	65.4	496	w			$\delta CC=O$ (30), δCOO (21), νCC (11)
$\delta CC=O$	A_g	457	5.1			498	m	$\delta CC=O$ (31), δCOO (20), δNCC (13)
δNCC	B_u	269	119.3					δNCC (58), δCCO (35), $\nu H…O$ (19)
δNCC	A_g	269	0.1			296	m	δNCC (53), δCCO (42), $\delta C=O…H$ (17)
τCN	B_g	167	0.1			178	m	τCN (56), τCC (13)
τCN	A_u	166	0.1					τCN (54), τCC (15)
$\delta C=O…H$	A_g	114	0.3			135	m	$\delta C=O…H$ (48), $\nu H…O$ (33)
$\tau C=O$	B_g	98	0.4					$\tau C=O$ (76), $\tau C–O$ (19)
$\nu H…O$	A_g	95	0.0					$\nu H…O$ (55), $\delta C=O…H$ (26)
$\tau C=O$	A_u	80	6.4					$\tau C=O$ (18), τCC (31), τCN (26), $\tau C–O$ (13)
$\nu H…O$	B_u	78	20.0					$\nu H…O$ (81), δCCO (15)
τCC	B_g	61	0.1					τCC (50), τCN (32)
τCC	A_u	51	4.9					τCC (33), $\tau C=O$ (26), τCN (19), δ_{op}(ring) (11)
δ_{op}(ring)	A_u	39	37.5					δ_{op}(ring) (41), τCC (32), τCN (11), $\tau C–O$ (10)

[a]Wavenumber values are in cm^{-1}. IR int. (infrared intensities) km·mol^{-1} and R int. (Raman scattering activities) in Å^4/amu. ν, stretching; δ, bending; ω, wagging; ρ, rocking; tw, twisting; τ, torsion; s, symmetric; as, asymmetric. The experimental intensities are only qualitative. PED: The number in parentheses is the percent contribution of each internal mode for the total potential energy. Contributions < 10% are not shown. When only one internal mode in the PED have a contribution > 10%, its value is ommited.

Raman spectrum of the later compound (A_g mode). The appearance of the doublet of bands in the Raman spectrum is probably due to a Fermi resonance involving the carbonyl stretching fundamental and the first overtone of the C–C stretching mode (A_g symmetry) whose fundamental vibration leads to the intense Raman band at 860 cm^{-1}. As is commonly observed [27–31], the calculations considerably overestimate the frequency of the νC=O mode, since they do not fully account for intermolecular effects that tend to reduce the frequency of this vibration (for glycine, polarization effects due to matrix/solute interactions [27–29] were not considered, while interdimer interactions [30,31] were neglected in the acid salt). In the case of the glycine acid salt, however, comparison of predicted frequencies for νC=O calculated using monomer and dimer 'models' (see Tables 5 and 6) clearly shows that the calculated frequency for this mode is considerably improved in the later, where intermolecular association is partially considered.

As with the νC=O mode, the calculations also overestimate the frequency of the antisymmetrical COO$^-$ stretching mode of the zwitterionic form and of the alkaline salt, while they underestimate the frequencies of the symmetrical COO$^-$ stretching vibration (see Tables 2 and 4). This results could be anticipated, since the calculations (for isolated molecules) do not take properly into account intermolecular interactions acting in the crystalline state that tend to make the two C–O bonds more similar and, thus, lead to an increase of the ν_sCOO$^-$ and decrease of ν_{as}COO$^-$ mode frequencies [30–32]. The assignment of the COO$^-$ stretching modes is made easier because these vibrations are predicted by the calculations to give rise to very intense infrared bands, whose counterparts in the Raman spectra are relatively weak.

The NH$_2$ and NH$_3$ bending modes were assigned easily, despite, in general, that some of the bands originated in these vibrations cannot be observed in the infrared spectra due to extensive overlap with the very intense ν_{as}COO band (they are, however, clearly observed in Raman).

The assignment of the CH$_2$ scissoring band does not present any major difficulty in the spectra of glycine and is ascribed to the infrared band at 1428 cm^{-1} for the neutral form and to the doublet at 1460

and 1444 cm^{-1} (1462 and 1446 cm^{-1} in the Raman spectrum) for the zwitterion. In the alkaline salt, this mode gives rise to the infrared band at 1431 cm^{-1} and to the Raman doublet at 1439 and 1410 cm^{-1}, while in the acid salt it gives the band at 1421 cm^{-1} (both in the infrared and Raman spectra).

Because carboxylic acid group intra-dimer interactions in the acid salt of glycine considerably increase the double bond character of the C–O(H) bond when compared with a pure carboxylic acid moiety, the νC–O vibration in this molecule occurs at a much higher frequency than in the isolated neutral form of glycine. We assign the infrared band at 1437 cm^{-1} (Raman: 1445 cm^{-1}) of the acid salt to this mode (infrared, B_u mode; Raman, A_g mode), while in the MI-IR spectrum of the neutral form of glycine this mode gives rise to the band at 1100 cm^{-1}. The corresponding calculated values for this mode are: glycine acid salt: 1464 cm^{-1} (A_g mode), 1461 cm^{-1} (B_u mode); neutral glycine: 1165 cm^{-1}). Note that as with the remaining C–O stretching modes, the predicted frequencies are overestimated by the calculations.

3.3. Region 1400–800 cm^{-1}

Most of the bands in this region are due to the wagging, twisting and rocking modes of the CH$_2$, NH$_2$ and NH$_3$ groups. When the CH$_2$ group is placed in an adjacent position to the NH$_2$ or NH$_3$ fragments, the vibrations become strongly coupled. This is reflected in the extensive mixing of these coordinates in the potential energy distribution calculated for most of these modes (see Tables 2–6).

For molecules containing the carboxylic acid group, the band due to δCOH can also be found in this spectral region (as usual, strongly coupled with νC–O [28–32], and also with ωCH$_2$). As previously referred, νC–O in neutral glycine also gives rise to a band in this region (1100 cm^{-1}), which is easily identified by taking into consideration its high intensity (see Table 3 and Fig. 3).

Finally, the νCC and νCN modes also give rise to bands in this region and are predicted by the calculations to be very sensitive to the nature of the neighbouring groups. Interestingly, these stretching vibrations seem to couple extensively only in the acid salt. Calculated frequencies and intensities are

in general good agreement with the experimental infrared and Raman data.

3.4. Region below 800 cm^{-1}

The deformation modes involving the skeletal atoms (δCOO, ωCOO, δCC=O and δNCC) appear in this spectral region, along with the torsional vibrations. The frequencies predicted for these vibrations (in particular τC–O and ωCOO) in the acid salt, on the basis of the dimer 'model' calculation, are in much better agreement with experimental data than those calculated using the monomer. The appearance of the band at 135 cm^{-1} in the Raman spectrum of this molecule, which was assigned to the δC–O...H 'ring' mode, is also worth noting. This could not be interpreted on the basis of the monomer 'model' calculation.

The predicted frequency for the NCC bending mode in the acid salt is 269 cm^{-1} (for both B_u and A_g modes). Thus, we assigned the Raman band at 296 cm^{-1} to this mode. In the zwitterionic glycine, this vibration is predicted to occur at a higher frequency than in the acid salt (calculated value: 320 cm^{-1}) and is here assigned to the Raman band at 364 cm^{-1}, whose infrared counterpart occurs at 358 cm^{-1} [9]. The τC–N mode (calculated value: 206 cm^{-1}) was previously assigned to the infrared band at ca. 520 cm^{-1} (Raman: 509 cm^{-1}), on the basis of neutron diffraction studies. Hence, it can be concluded that intermolecular interactions within the crystal significantly affect the frequency of this vibration relative to the value obtained for the simple isolated molecule 'model' used here. It should be pointed out that the failure of theoretical predictions using simple isolated molecule 'models' for torsional vibrations in crystals, has already been indicated for other molecules [32] and should be taken into consideration using this kind of approach.

4. General conclusions

Following from extensive comparisons between theoretical predictions and spectroscopic data (FT-IR, Raman and MI-IR) for neutral and zwitterionic forms of glycine, the ab initio theoretical vibrational calculations here presented for the acid and alkaline salts

of glycine, using a moderate basis set (6-31G*) at the Hartree–Fock level of theory, produce helpful predictions of vibrational frequencies for the assignment of the vibrational spectra of these molecules. In addition, although generally not as accurate as the frequencies, the theoretically predicted intensities (both in infrared and in Raman) have proved useful in assignment of the spectra. Finally, a dimeric structure of the acid salt of glycine in the crystalline state was found to give best results in the prediction of the vibrational spectra of this compound.

Acknowledgements

References

[1] J.H. Caldwell, N.W. Daw, H.J. Wyatt, J. Physiol. 276 (1978) 277.

[2] S. Suzuki, T. Shimanouchi, M. Tsuboi, Spectrochim. Acta 19A (1963) 1195.

[3] S.F.A. Kettle, E. Lugwisha, J. Eckert, N.K. McGuire, Spectrochim. Acta 45A (1989) 533.

[4] R.W. Williams, V.F. Kalasinsky, A.H. Lowrey, J. Mol. Struct. 281 (1993) 157.

[5] B. Depuy, C. Garrigou-Lagrange, J. Chim. Phys. 65 (1968) 450.

[6] C. Destrade, C. Garrigou-Lagrange, M.-T. Forel, J. Mol. Struct. 10 (1971) 203.

[7] T.C. Cheam, J. Mol. Struct. 274 (1972) 289.

[8] Y. Ding, K. Krogh-Jesperssen, J. Comput. Chem. 17 (1996) 338.

[9] K. Furic, V. Mohacek, M. Bonifacic, I. Štefanic, J. Mol. Struct. 267 (1992) 39.

[10] E.D. Radchenko, G.G. Sheina, N.A. Smorygo, Yu.P. Blagoi, J. Mol. Struct. 116 (1984) 386.

[11] A. Vijay, D.N. Sathyanarayana, J. Phys. Chem. 96 (1992) 10735.

[12] A.H. Lowrey, V.F. Kalasinsky, R.W. Williams, Struct. Chem. 4 (1993) 289.

[13] Y. Ding, K. Krogh-Jesperssen, Chem. Phys. Lett. 199 (1992) 261.

[14] P.-G. Jönsson, Å. Kvick, Acta Cryst. 28B (1972) 1827.

[15] M.J. Frisch, G.W. Trucks, H.B. Schlegel, P.M.W. Gill, B.G. Johnson, M.W. Wong, J.B. Foresman, M.A. Robb, M. Head-Gordon, E.S. Replogle, R. Gomperts, J.L. Andres, K. Raghavachari, J.S. Binkley, C. Gonzalez, R.L. Martin, D.J. Fox, D.J. Defrees, J. Baker, J.J.P. Stewart, J.A. Pople, Gaussian 92/DFT, Revision G.3, Gaussian, Pittsburgh, PA, 1993.

[16] W.J. Hehre, R. Ditechefield, J.A. Pople, J. Chem. Phys. 56 (1972) 2257.

[17] H.B. Schlegel, Ph.D. Thesis, Queen's University, Kingston, Ontario, Canada, 1975.

[18] R. Fausto, TRANSFORMER (version 2.0), Departamento de Química, Universidade de Coimbra, Portugal, 1997.

[19] M.D.G. Faria, R. Fausto, BUILD-G (version 2.0) and VIBRAT (version 2.0), Departamento de Química, Universidade de Coimbra, Portugal, 1997.

[20] H. Fuher, V.B. Kartha, K.G. Kidd, P.J. Krueger, H.H. Mantsch, Natl. Res. Council Can. Bull. 15 (1976) 1.

[21] J.R. Durig, Invited Oral Presentation in the NATO-ASI Conference on Low Temperature Molecular Spectroscopy, Ponta Delgada, Portugal, 1995.

[22] H. Susi, D.M. Byler, J. Mol. Struct. 63 (1980) 1.

[23] S. Bratoz, D. Hadzi, N. Sheppard, Spectrochim. Acta 8A (1956) 249.

[24] R.K. Khanna, M. Horak, E.R. Lippincott, Spectrochim. Acta 22A (1966) 1759.

[25] R.S. Krishnan, K. Krishnan, Proc. Indian Acad. Sci. 60 (1964) 11.

[26] N.D. Sokolov, Ann. Chim. 10 (1965) 497.

[27] A. Kulbida, R. Fausto, J. Chem. Soc. Faraday Trans. 89 (1993) 4257.

[28] A. Kulbida, M.N. Ramos, M. Rasanen, J. Nieminen, O. Schrems, R. Fausto, J. Chem. Soc. Faraday Trans. 91 (1995) 1571.

[29] R. Fausto, A. Kulbida, O. Schrems, J. Chem. Soc. Faraday Trans. 91 (1995) 3755.

[30] R. Fausto, P.J. Tonge, P.R. Carey, J. Chem. Soc. Faraday Trans. 90 (1994) 3491.

[31] R. Fausto, J. Mol. Struct. 377 (1996) 181.

[32] R. Fausto, Ph.D. Thesis, Departamento de Química, Universidade de Coimbra, Portugal, 1988.